Materials Science and Engineering B 174 (2010) 269–272

Contents lists available at ScienceDirect

Materials Science and Engineering B

journal homepage: www.elsevier.com/locate/mseb

AC and dielectric properties of vacuum evaporated InTe bilayer thin films

P. Matheswaran[a], R. Sathyamoorthy[a,*], R. Saravanakumar[a], S. Velumani[b]

[a] PG and Research, Department of Physics, Kongunadu Arts and Science College (Autonomous), GN Mills (po), Coimbatore 641 029, Tamil Nadu, India
[b] Department of Electrical Engineering (SEES), CINVESTAV-IPN Zacatenco, D.F., 07360, Mexico

ARTICLE INFO

Article history:
Received 31 August 2009
Received in revised form
21 December 2009
Accepted 4 March 2010

Keywords:
InTe bilayer thin film
Thermal evaporation
Dielectric properties
AC conduction

ABSTRACT

III–VI compound semiconductors receive great attention due to its applications in memory devices, switching devices, gas sensors, hybrid solar cells, etc. InTe thin films were prepared by sequential thermal evaporation of In and Te at Ar atmosphere. X-ray diffraction pattern of the films shows that the films posses mixed phase of In_2Te_3 and In_2Te_5. Grain size (D) and dislocation density were calculated by using Scherer's formula. Surface morphology of the film is analyzed by SEM and the surface is found to be agglomeration of well defined grains. EDS analysis reveals that elemental composition is in right stoichiometry. The value of capacitance and tan δ was recorded with respect to different frequencies and at different temperatures. It is observed that the capacitance decreases with increase in frequency at all temperatures. The observed nature of the capacitance is due to the inability of the dipoles to orient in a rapidly varying electric field. The pronounced increase in capacitance toward the low frequency region may be attributed to the blocking of charge carriers at the electrodes which leads to space charge layer resulting in the increase of capacitance. The mechanism responsible for AC conduction is found to be electronic hopping. TCC and TCP values were calculated and the results are discussed.

1. Introduction

III–VI semiconducting compounds are receiving great technological interest because of their interesting electrical and optical properties [1–5]. Among these compounds, indium telluride (In_2Te_3) is a well known semiconductor for radiation detector, switching and photovoltaics [6–9]. Indium telluride is a direct band gap semiconductor with the band gap energy of 1.1 eV. In_2Te_3 posses two structural modifications namely α and β. Both the structural modifications having one-third or two-third of indium sub-lattices remain vacant. This kind of neutral impurities plays a major role in describing the structural, optical and electrical conductivity of the film. Many workers investigated the structural, optical and electrical properties of bulk In_2Te_3 [10–13]. Conduction mechanism in amorphous In_2Te_3 thin films has been reported by Hegab and Bekheet [14]. Growth and electrical transport properties of InTe thin film have been reported by Mathur et al. [15], but no work has been carried out on electrical characterization of In/Te bilayer thin film prepared by sequential thermal evaporation. In the present work, an attempt has been made to prepare In_2Te_3 thin film from In/Te bilayer by sequential thermal evaporation and to investigate their structural, dielectric and AC conduction properties at various temperatures.

2. Experimental details

In_2Te_3 bilayer thin films were prepared on to well cleaned glass substrates by sequential thermal evaporation of In and Te using 5N pure powder materials (Sigma–Aldrich Chemicals, US) under a base pressure of 1×10^{-5} mbar in Ar atmosphere. The thickness of both layers In and Te was chosen in order to get effective mixing with atomic proportions. In order to compensate the re-evaporation of chalcogenide during annealing, we have taken the thickness ratio of Te/In was slightly higher than 3/2 to form In_2Te_3. The thickness of the films was monitored and controlled by Quartz Crystal thickness monitor. Bottom and top electrode is used to sandwich the InTe thin film with Al as the electrode material. Al/InTe sandwich thin film system was annealed at 300 °C in Ar atmosphere for half an hour in order to form InTe. Complete system of Al/InTe/Al is prepared by thermal evaporation technique with individual elements. Temperature was measured by chromel–alumel thermocouple. X-ray diffraction studies were carried out using PANalytical instrument with CuKα radiation in order to get structural information. Surface morphology and elemental composition of the films were analyzed by scanning electron microscopy and energy dispersive X-ray spectroscopy, respectively. With the help of digital LCR meter (LCR-819, GW Instek, Good will Instrument Ltd., Taiwan), measurements of series capacitance and the dissipation factor for different frequen-

* Corresponding author. Tel.: +91 0422 2642095x251; fax: +91 0422 2644452.
E-mail address: rsathya59@gmail.com (R. Sathyamoorthy).

0921-5107/$ – see front matter
doi:10.1016/j.mseb.2010.03.008

Table 1
Structural parameters of InTe thin film.

Film thickness (Å)	FWHM	Strain ($\times 10^{-2}$ dyn/cm^2)	Dislocation density ($\times 10^{18}$)	Crystalline size (nm)
4000	0.20468	5.01397	1.91551	72.2

cies were carried out at various temperatures (291–448 K) under vacuum of 10^{-3} mbar. All the experiments were repeated three times in order to check the reproducibility and the error bar was about ±2%. The dielectric constant (ε') was evaluated from the observed capacitance data. The parallel equivalent conductance ($Gp = \omega Cp \tan\delta$) was calculated at different temperatures.

3. Results and discussion

3.1. Structural properties

Fig. 1 represents the XRD spectra of indium telluride thin film of typical thickness 4000 Å. From Fig. 1, it is observed that the structure of the film contains the mixed phase of In_2Te_3 and In_2Te_5 (JCPDS 16-0445 & 71-0109). In_2Te_3 phase of the film exhibits with the preferential orientation along (5 1 1), (6 6 0) and (7 7 1) plane at 2θ equal to 23°, 40.3° and 49°, respectively, whereas In_2Te_5 phase exhibits with the preferential orientation along (4 4 0) plane and (6 2 2) plane at 2θ equal to 27° and 33°, respectively. From Fig. 1, it is inferred that the films contain mixed phase of In_2Te_3 and In_2Te_5; whereas In_2Te_5 phase is dominant when it is compared with In_2Te_3 phase. The electronegativity difference between the metal and the chalcogene is quite small, since the electronegativity of tellurium and indium is 2.1 and 1.7, respectively. This small electronegativity difference induces a poor stability of such compounds, whose composition that depends strongly on preparation condition and annealing temperature. The grain size (D) of the dominant phase was calculated by using Scherer's formula and it is given in Table 1.

Fig. 2 represents the SEM image of InTe thin film. The SEM images clearly denote that the film have homogeneous surface without any pinhole. The grains tend to agglomerate with nearer grains to form bigger grains, which supports the XRD result [16]. Spherical geometry of the grains was vanished due to agglomeration of grains, thereby reducing grain boundaries. Table 2 shows the elemental composition of the InTe thin film. It is observed that excess in tellurium content implies that the possibility of existence of In_2Te_5 phase along with In_2Te_3 phase [1]. This also supports the XRD results.

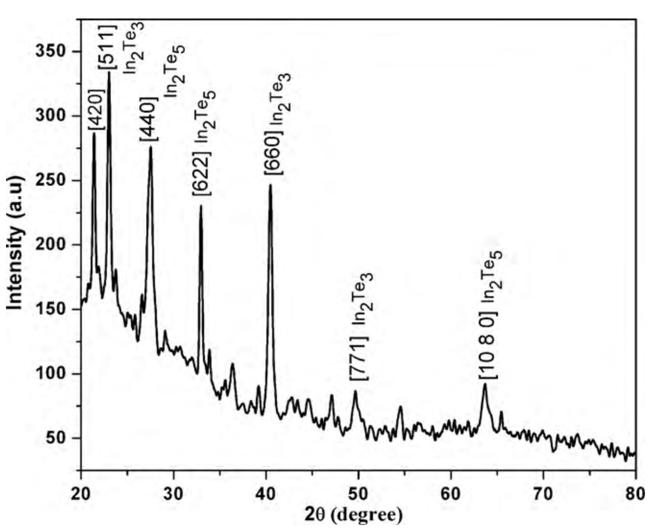

Fig. 1. XRD spectra of InTe thin film.

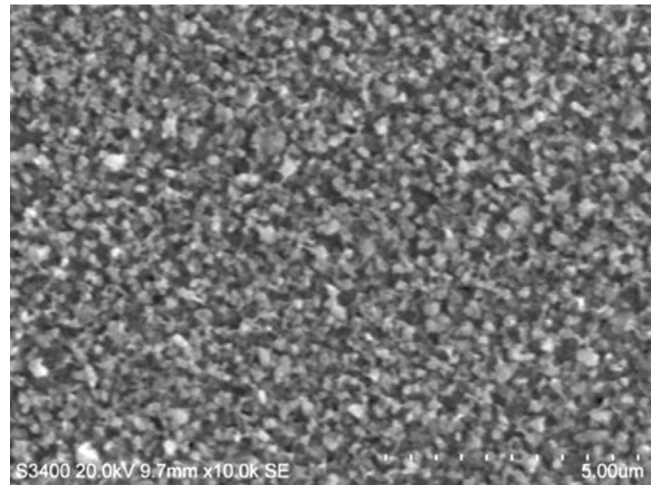

Fig. 2. SEM image of InTe thin film.

Table 2
Elemental composition of InTe film.

Film thickness (Å)	Element	Atomic %
4000	In	34
	Te	66

3.2. Dielectric properties

The variation of capacitance with frequency in the frequency range 100 Hz to 60 kHz for different temperatures is shown in Fig. 3. The capacitance decreases with increase in frequency. It may be due to the screening of the electric field across the film by charge redistribution [17–19]. At low frequencies, the charges on neutral impurity defects are more readily redistributed, such that defects closer to the positive side of the applied field become negatively charged while the defects closer to the negative side of

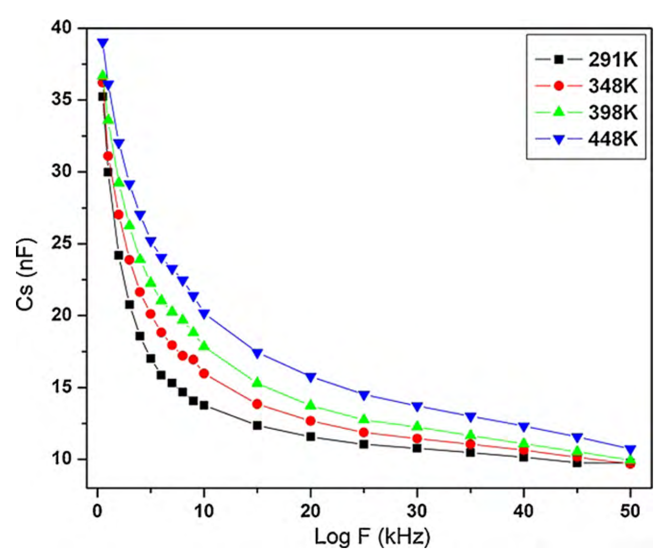

Fig. 3. Variation of Cs with log frequency.

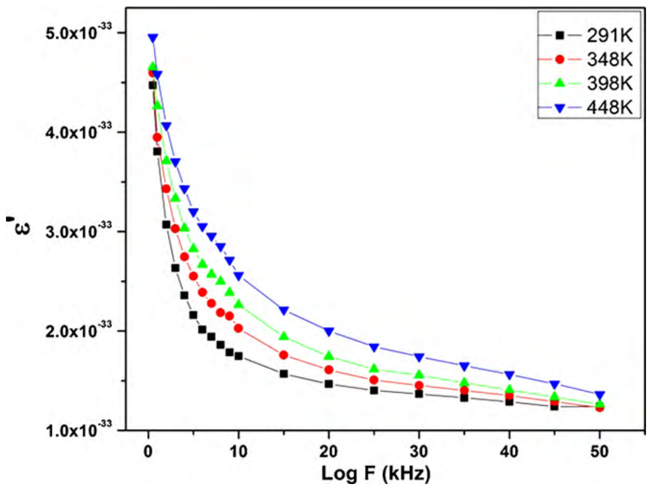

Fig. 4. Variation of ε' with log frequency.

the field become positively charged. As the frequency is increased, the capacitance decreases to the same limit, as the charges on the defects no longer have time to rearrange in response to the applied voltage. At higher temperature, the screening is more effective, because of the increase in thermal activation of charges as observed [20].

Fig. 4 presents the dependence of dielectric constant (ε') with frequency. The dielectric constant also decreases with increase in frequency at all temperatures exhibiting a similar trend as that of the capacitance. These curves closely resemble those predicted by the Debye relaxation model for orientational polarization [21]. Fig. 5 shows the typical variation of $\tan\delta$ with frequency at various temperatures. The loss factor is found to increase with increase in frequency, whereas it decreases with increase in temperature, which may be due to the effect of lead resistances.

Temperature dependence of the capacitance (TCC) and temperature dependence of permittivity for different frequencies have been shown in Figs. 6 and 7, respectively. The capacitance was found to increase with increasing temperature. The temperature co-efficient of capacitance (TCC) and permittivity (TCP) have been evaluated using the expressions:

$$\mathrm{TCC} = \left(\frac{1}{\mathrm{Cs}}\right) \times \left(\frac{dC}{dT}\right) \tag{1}$$

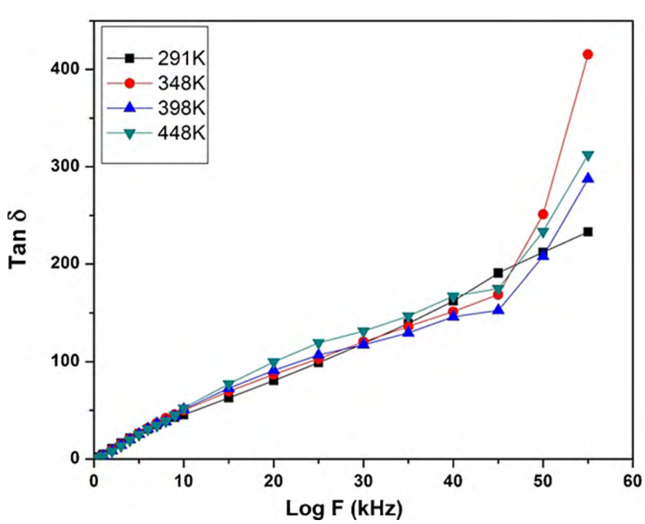

Fig. 5. Variation of dielectric loss with log frequency at different temperatures.

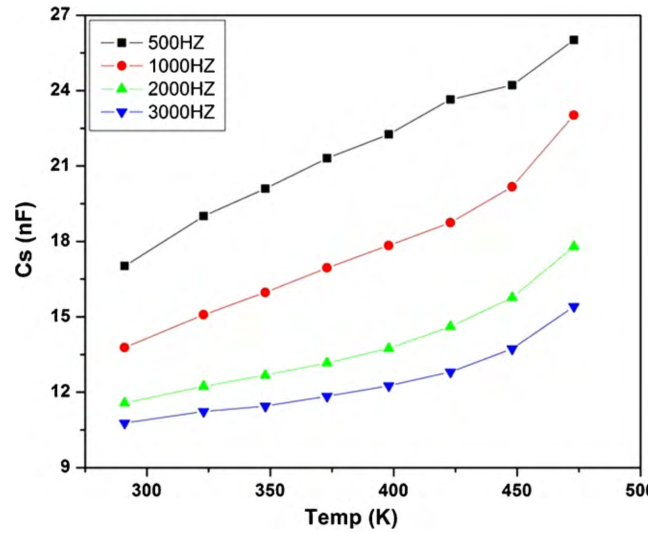

Fig. 6. Variation of capacitance with temperature.

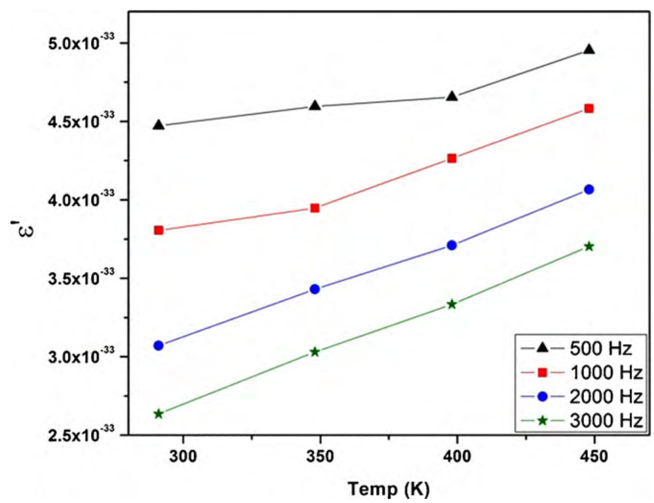

Fig. 7. Variation of ε' with temperature.

$$\mathrm{TCP} = \left(\frac{1}{\varepsilon'}\right) \times \left(\frac{d\varepsilon'}{dT}\right) \tag{2}$$

Table 3 summarizes the estimated values of TCC and TCP for different frequencies. It is found that the TCC values increase with frequency and TCP values decrease with increase in frequency. This effect may be attributed to the electron hopping between the pair of centres under the action of alternating current field which is equivalent to the reorientation of the dipoles. Hence the variation of TCP and TCC is attributed to the presence of dipoles [22,23].

3.3. AC conduction properties

The AC conductance (Gp) was calculated at different temperatures from the measured values of capacitance and loss factor.

Table 3
Frequency dependence of TCC and TCP.

S. No.	Frequency (Hz)	TCC (ppm/K $\times 10^{-4}$)	TCP (ppm/K)
1	500	5.33	1.51996
2	1000	1666.63	0.951998
3	2000	4166.70	0.666670
4	3000	5553.00	0.606078

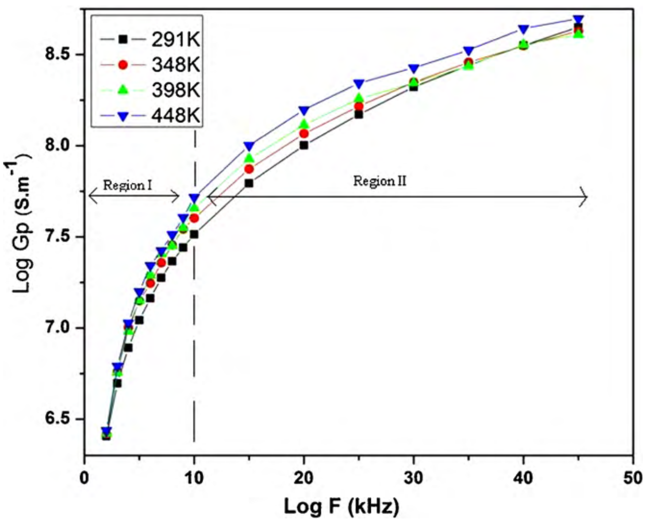

Fig. 8. Dependence of AC conductance with frequency.

The plot of AC conductance versus frequency for different temperatures is shown in Fig. 8. The AC conductance has been found to vary according to the relation Gpαf^n, where the value of n depends on the temperature and frequency. The curves exhibit two dispersion regions one below 10 kHz and the other above 10 kHz. At room temperature, n values range from 0.7 to 0.9. In the second region (>10 kHz), nearly all the curves approximate to a square law dependence on frequency and show less dependence at higher frequencies. AC conductivity increases with frequency as long as the frequency of the field is lower than the charge carrier jump in the solid [24].

The strong frequency dependence at high frequencies suggests the electronic hopping mechanism for the conduction. A similar behavior has been observed by various investigators on insulating dielectric thin films [25–27]. In the first region (<10 kHz), the slopes of the curves are less than two and are found to be temperature sensitive. When the temperature increases, the value of n decreases. Jonscher [28] accounted for this behavior on the basis of easy and difficult hopes of the carriers between the possible sites. The contributions to conductivity from the carrier movement (carrier movement between and within the defect wells) at different temperatures are different, thereby resulting in the decrease of n with increase of temperature. This phenomenon suggests that the mechanism responsible for AC conduction is electronic hopping [28,29].

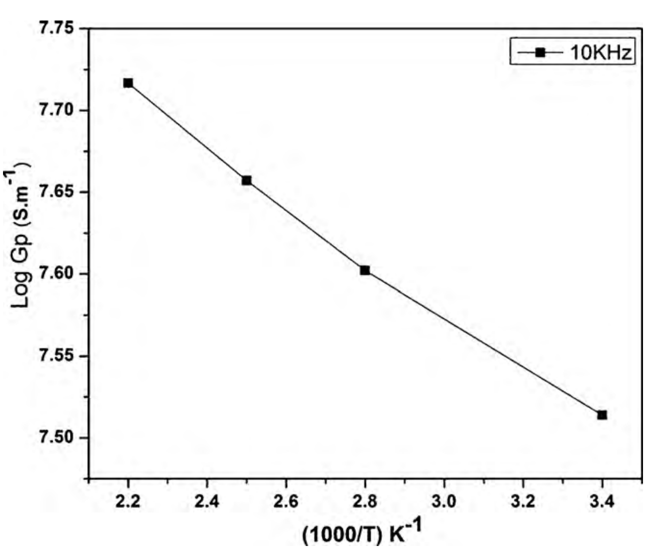

Fig. 9. Variation of AC conductance with temperatures.

Fig. 9 exhibits the temperature dependence of AC conductance and the estimated activation energy is 0.07326 eV. The observed low value of activation energy suggests that the conduction mechanism in these films may be due to the hopping of electrons, which is in accordance with earlier investigations on other semiconducting films [30,31].

4. Conclusion

Indium telluride thin film system was prepared on cleaned glass substrate by sequential thermal evaporation and post-deposition annealing at 300 °C in Ar atmosphere for half an hour. Structural analysis shows that the film contains the mixed phase of In_2Te_3 and In_2Te_5. The capacitance and loss factor are dependent on both temperature and frequency. The dielectric constant (ε'), temperature co-efficient of capacitance (TCC) and temperature co-efficient of permittivity (TCP) were estimated. The process of AC conduction has been explained on the basis of hopping mechanism. The mechanism responsible for AC conduction is electronic hopping.

Acknowledgement

The author greatly acknowledges the Inter University Accelerator Centre, New Delhi for providing the UFUP - 40304 project to carry out the research work.

References

[1] N. Guettari, C. Amory, M. Morsli, J.C. Bernede, A. Khelil, Thin solid films 431–432 (2003) 497–501.
[2] R. Rousina, G.K. Shivakumar, Surf. Coat. Technol. 38 (1989) 353–358.
[3] M.A.M. Seyam, Appl. Surf. Sci. 181 (2001) 128–138.
[4] J.C. Woolley, B.I. Pamplin, J.A. Evans, J. Phys. Chem. Solids 19 (1961) 147–154.
[5] L.A. Franks, B.A. Brunett, R.W. Olsen, D.S. Walsh, G. Vizkelethy, J.I. Trombka, B.L. Doyle, R.B. James, Nucl. Instrum. Meth. A 428 (1999) 95–101.
[6] L.A. Franks, B.A. Brunett, R.W. Olsen, D.S. Walsh, G.K. Vizkelethy, J.I. Trombka, B.L. Doyle, R.B. James, Nucl. Instrum. Meth. A 428 (1999) 95–101.
[7] J.R. Woodyard, G.A. Landis, Sol. Cells 31 (1991) 297–329.
[8] M.A. Afifi, N.A. Hegab, A.E. Bekheet, Vacuum 47 (1996) 265–269.
[9] I.N. Volovichev, Yu.G. Gurevich, V.M. Koshkin, Microelectron. J. 29 (1998) 535–542.
[10] M. Emziane, J.C. Bernede, J. Ouerfellia, H. Essaidi, A. Barreau, Mater. Chem. Phys. 61 (1999) 229–236.
[11] R.R. Desai, D. Lakshminarayana, P.B. Patel, P.K. Patel, C.J. Panchal, Mater. Chem. Phys. 94 (2005) 308–314.
[12] D.V. KrishnaSastry, P. Jayarama Reddy, Solid State Commun. 45 (1983) 199–201.
[13] S.R. Ovshinsky, Phys. Rev. Lett. 21 (1968) 1450–1453.
[14] N.A. Hegab, A.E. Bekheet, J. Mater. Sci. 36 (2001) 3817–3823.
[15] P.C. Mathur, A. Kumar, O.P. Taneja, A.L. Dawar, Thin Solid Films 78 (1981) 377–383.
[16] S. Lalitha, R. Sathyamoorthy, S. Senthilarasu, A. Subbarayan, K. Natarajan, Sol. Energ. Mater. Sol. C 82 (2004) 187–199.
[17] P.W. Zukowski, S.B. Kantorow, D. Maczka, V.F. Stelakh, Phys. Stat. Sol. A 112 (1989) 695–698.
[18] A. Vasudevan, S. Carin, M.R. Melloch, E.S. Harmon, Appl. Phys. Lett. 73 (1998) 671.
[19] H.M. Lin, Y.F. Chen, J.L. Shen, C.W. Chou, Appl. Phys. Lett. 78 (13) (2001) 1909.
[20] M.D. Kannan, S.K. Narayandass, C. Balasubramanian, D. Mangalaraj, Phys. Stat. Sol. A 121 (1990) 515–522.
[21] H. Birey, J. Appl. Phys. 49 (1978) 2898.
[22] S.S. Bharadwaja, S.B. Krupanidhi, Mater. Sci. Eng. B 78 (2000) 75.
[23] K. Prabakar, Sa.K. Narayandass, D. Mangalaraj, Mater. Chem. Phys. 78 (2003) 809–815.
[24] J.C. Dyre, J. Appl. Phys. 64 (1988) 2456.
[25] W.S. Chan, A.K. Jonscher, Phys. Stat. Sol. 32 (1969) 749.
[26] F. Argall, A.K. Jonscher, Thin Solid Films 2 (1968) 185.
[27] B.G. Sealy, A.J. Crocker, M.J. Lee, R.F. Egerton, Thin Solid Films 11 (1972) 365–376.
[28] A.K. Jonscher, J. Non-Cryst. Solids 8 (1972) 293–315.
[29] J. Dheepa, R. Sathyamoorthy, A. Subbarayan, S. Velumani, P.J. Sebastian, R. Perez, Sol. Mater. Sol. C 88 (2005) 187.
[30] N. Croitora, N. Marinescu, Phys. Rev. 9 (1964) 202.
[31] P.A. Walley, Thin Solid Films 2 (1968) 327–336.